Improving Continual Learning by Accurate Gradient Reconstructions of the Past

Anonymous authors
Paper under double-blind review

Abstract

Regularization and experience replay are two popular continual-learning strategies with complementary strengths: while regularization requires less memory, replay can more accurately mimic batch training. But can we combine them to get better methods? Despite the simplicity of the question, little is known or done to optimally combine these approaches. In this paper, we present such a method by using a recently proposed principle of adaptation that relies on a faithful reconstruction of the gradients of the past data. Using this principle, we design a prior which combines two types of replay methods with a quadratic weight-regularizer and achieves better gradient reconstructions. The combination improves performance on standard task-incremental continual learning benchmarks such as Split-CIFAR, SplitTinyImageNet, and ImageNet-1000, achieving $>80\%$ of the batch performance by simply utilizing a memory of $<10\%$ of the past data. Our work shows that a good combination of replay and regularizer-based methods can be very effective in reducing forgetting, and can sometimes even completely eliminate it.

1 Introduction

Continual learning (Parisi et al., 2019) aims for accurate incremental training over a large number of individual tasks/examples. This can potentially reduce the frequency of retraining in deep learning, making algorithms easier to use and deploy, while also reducing their environmental impact (Diethe et al., 2019; Paleyes et al., 2020). The main challenge in continual learning is to remember past knowledge and reuse it to continue to adapt to new data. This can be difficult because the future is unknown and can interfere with past knowledge (Sutton, 1986; Mermillod et al., 2013; Kirkpatrick et al., 2017). Performance, therefore, heavily depends on the strategies used to represent and reuse past knowledge.

Two popular strategies of knowledge reuse are based on regularization and experience replay and have complementary strengths. For example, the well-known Elastic-Weight Consolidation (EWC) (Kirkpatrick et al., 2017), which regularizes the new weight-vector to keep it close to the old one, is compact and requires storing only two vectors, one containing the weights and the other their importance (often the empirical Fisher). A variety of other such regularizers have been proposed (Schwarz et al., 2018; Zenke et al., 2017; Li & Hoiem, 2017; Nguyen et al., 2018), and are usually motivated as treating parameters in a Bayesian fashion. This is very different from experience replay (Robins, 1995; Shin et al., 2017), where past examples are simply added during future training. Memory cost here can be substantial, but it can boost accuracy if the memory represents the past well. Clearly, combining the two approaches can strike a good balance between performance and memory size.

At present, little has been done to find principled ways to combine regularization and experience replay. Some works have used knowledge distillation (Rebuffi et al., 2017; Buzzega et al., 2020) or functional regularization (Titsias et al., 2020; Pan et al., 2020), where predictions evaluated at the examples in memory are regularized. Such approaches are promising, but it is not clear why the specific choices of regularizers and memory work well, and whether there are better choices that lead to further improvements.

In this paper, we provide a theoretically-motivated approach to combine and improve regularization and experience replay. Our approach is based on a recently proposed principle of adaptation (Khan & Swaroop,

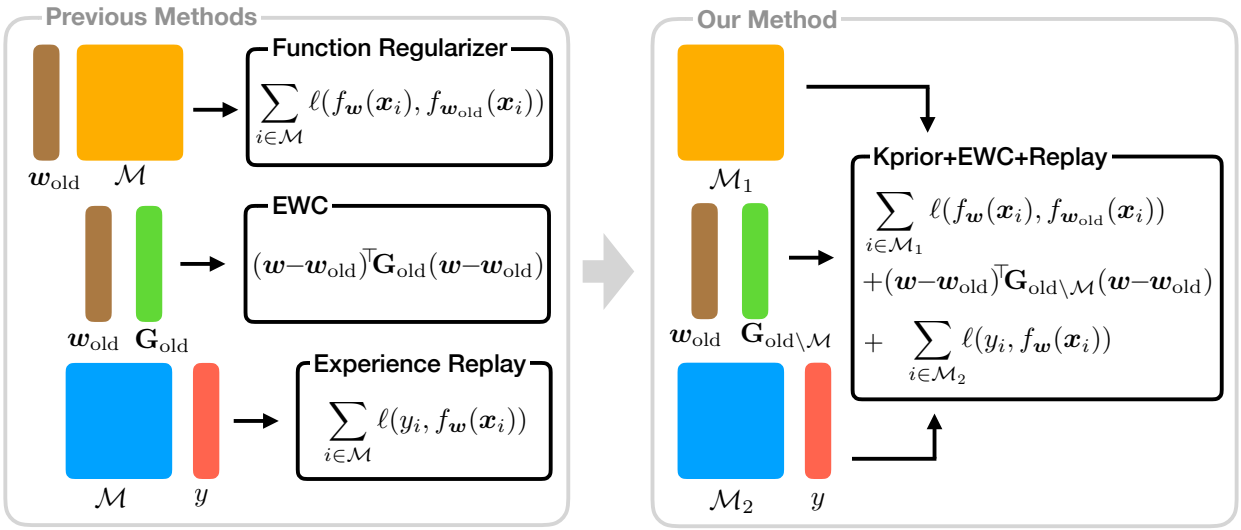

Figure 1: Using the principle of gradient reconstructions, we design a new prior (right) to combine different types of regularization and memory-based methods. EWC uses a quadratic regularizer based on the old weight-vector and its importance, while experience replay uses a memory of past examples along with their labels. Function regularization often does not require the labels, but also lacks a weight regularizer. Our method combines these different types of methods, using two memory sets, $\mathcal{M}_1 \cup \mathcal{M}_2 = \mathcal{M}$. The notable differences are that our method's importance matrix excludes the examples in the entire memory set $\mathcal{M}$, and that experience replay is applied only to the second memory set $\mathcal{M}_2$. The examples in the first memory set $\mathcal{M}_1$ do not require labels, and can be compressed to only keep a small set of representative inputs that may not be part of the old training sets. See Section 5 for details on our method and the choice of memory.

2021), where a prior called the Knowledge-adaptation prior (K-prior) is used to reconstruct the gradients of the past training objective. In the continual learning setting, this requires an accurate reconstruction of the gradients over all the past tasks, and can be used as a guideline to design better priors. Khan & Swaroop (2021) considered only one-task adaptation, and used a simple quadratic regularizer without any experience replay. We extend their method to multiple tasks and use it to combine different regularization and replay methods. Using the principle of gradient reconstruction of the past, we design a prior that combines a weight-regularizer, a functional regularizer, and experience replay (Fig. 1). Each piece contributes in a new way to the reduction of a different type of error, and the combination overall gives lower gradient-reconstruction error than each individual component. This leads to consistent improvements on standard benchmarks for multi-task image classification in task-incremental continual learning, such as Split-CIFAR, Split-TinyImageNet, and ImageNet-1000, across various memory budgets from small to large sizes. This approach is theoretically-motivated and can yield better strategies than the current heuristics used in the literature.

2 Related work

Continual learning paradigms. Existing CL methods can be classified into three orthogonal / complimentary paradigms (which can be combined): 1) *weight-regularization-based methods* regularize parameter updates by penalizing changes in 'important' parameters for previous tasks, 2) *memory/rehearsal-based methods* rehearse some past data or pseudo-data, and 3) *architecture-based methods* change the model architecture or mask model weights (Parisi et al., 2019; Swaroop, 2022). Here, we focus on the first two CL paradigms. Weight-regularization-based approaches include Elastic Weight Consolication (EWC) (Kirkpatrick et al., 2017), Online EWC (Schwarz et al., 2018), Synaptic Intelligence (SI) (Zenke et al., 2017), Learning without Forgetting (LwF) (Li & Hoiem, 2017), and Variational Continual Learning (VCL) (Nguyen et al., 2018). Memory/rehearsal-based approaches include (Experience) Replay (Robins, 1995) and Deep Generative Re-

play (DGR) (Shin et al., 2017). We will use memory via functional-regularization / distillation, sharing conceptual similarities to Functional Regularization for CL (FRCL) (Titsias et al., 2020), Functional Regularisation of Memorable Past (FROMP) (Pan et al., 2020), Incremental Classifier and Representation Learning (iCaRL) (Rebuffi et al., 2017), and Dark Experience Replay (DER) (Buzzega et al., 2020).

Function-space regularization methods for continual learning. Our method builds upon K-priors, which is closely related to function-space regularization methods for continual learning. FROMP (Pan et al., 2020) in particular is closely related to K-priors (Khan & Swaroop, 2021), as they both use similar forms for the functional divergence. Viewed from the perspective of K-priors, FROMP can be interpreted as a mechanism to reconstruct the gradient of the past, which leads to strong empirical performance (Pan et al., 2020). Another related method is FRCL (Titsias et al., 2020), which uses a GP-based formulation with inducing points to enable functional regularization for continual learning. However, as shown in (Pan et al., 2020), FROMP outperforms FRCL (see Pan et al. (2020) for a discussion on the key methodological differences between FROMP and FRCL). Finally, gradient episodic memory (GEM) (Lopez-Paz & Ranzato, 2017) is also closely related to K-priors and hence our work. In particular, GEM is conceptually similar to (Vapnik et al., 2015), which regularizes the loss of a student model using the output of a teacher model. Lopez-Paz & Ranzato (2017) formulates this in terms of the gradients using a dual approach. While this formulation is conceptually similar to K-priors, K-priors leverages a simpler first-order optimization method instead of the dual approach.

Continual learning settings. There are three distinct continual learning settings, which differ in whether for a given image at test time, the corresponding task identity is known, and, if not, whether the model is explicitly required to infer the task identity (Van de Ven & Tolias, 2019): 1) *task-incremental learning*, where the task identity is known, allowing us to have task-specific model components such as a multiple output heads; 2) *domain-incremental learning*, where the task identity is not known and the model is not required to infer the task identity, which is typically solved by single-headed architectures, and 3) *class-incremental learning*, where the task identity is not known and is required to be inferred by the model, which includes common real-world problems such as sequentially learning new object classes (Van de Ven & Tolias, 2019). In this work, we exclusively focus on task-incremental learning.

Knowledge-adaptation priors (K-priors) Khan & Swaroop (2021) is a principled, foundational approach for general, quick and accurate model adaptation that unifies and generalizes many previous methods. In addition to our main technical contribution of improving K-priors by correcting for two major sources of error, we substantially expand upon Khan & Swaroop (2021) in two aspects: 1) They only consider one-step adaptation settings (i.e. with 2 tasks). Alas, we will show that K-priors incur an error that accumulates as more tasks are met. This makes it especially important to assess more realistic CL scenarios with longer task sequences, which we do in this work (up to 10 tasks). 2) their experiments are limited to small-scale models and datasets, the largest only involving a small CNN (1.2M parameters) on CIFAR-10 (10 classes, 60K data points). In contrast, we demonstrate scalability up to a ResNet-18 (11M parameters) on ImageNet (1000 classes, 1.2M data points).

3 Continual learning methods

We focus on a continual learning (CL) problem to incrementally learn from a sequence of data sets $\mathcal{D}_1, \ldots, \mathcal{D}_T$, corresponding to a total of T tasks. This is different from the commonly used batch-training in deep learning, where data from all the tasks is assumed to be available at all times during training. CL is challenging as the model needs to repeatedly adapt to new tasks, while not forgetting previously-gathered knowledge. Our goal is to get the performance as close as possible to the model that is trained on data from all tasks.

Formally, consider a supervised learning problem with $\mathcal{D}_t$ containing N input-output pairs $(\boldsymbol{x}_i, y_i)$, with $\boldsymbol{x}_i \in \mathbb{R}^D$ and $y_i \in \mathcal{Y}$, and we wish to train a model with output $f_{\boldsymbol{w}}(\boldsymbol{x}_i)$ (also denoted as $f^i_{\boldsymbol{w}}$), and a P-length parameter $\boldsymbol{w}$ in a space $\mathcal{W} \subset \mathbb{R}^P$. Then, at any given task t, the best possible model parameters $\boldsymbol{w}^\star_t$ can be obtained by training on all the data examples $\mathcal{D}_{1:t} = \cup_{i=1}^t \mathcal{D}_i$, for example, by solving the optimization

problem shown below,

$$\boldsymbol{w}_t^\star = \arg\min_{\boldsymbol{w}\in\mathcal{W}} \ \ell_t^{\text{batch}}(\boldsymbol{w}), \tag{1}$$

$$\text{where} \quad \ell_t^{\text{batch}}(\boldsymbol{w}) = \sum_{i\in\mathcal{D}_{1:t}} \ell\big(y_i, \sigma(f_{\boldsymbol{w}}^i)\big) + \mathcal{R}(\boldsymbol{w}). \tag{2}$$

We assume the loss $\ell(y_i, \sigma(f_i))$ is defined through the log-likelihood of an exponential family distribution (e.g., cross-entropy), with $\sigma(f)$ being a transformation of the model outputs (e.g., softmax) defined using the link-function of the distribution. We denote a regularizer by $\mathcal{R}(\boldsymbol{w})$, and in what follows, we will use an L_2 regularizer $\mathcal{R}(\boldsymbol{w}) = \frac{1}{2}\delta\|\boldsymbol{w}\|^2$, with $\delta \geq 0$.

The main challenge in CL is to remember the useful past knowledge extracted from previous tasks $\mathcal{D}_{1:t-1}$, and reuse it during training over the new task $\mathcal{D}_t$ to get as close as possible to $\boldsymbol{w}_t^\star$. We would like a compact summary of the past knowledge, because we are not allowed to store all past data. We will now describe two strategies used in the literature, based on regularization and experience replay, and discuss the challenges in combining them.

Regularization-based approaches aim to keep the new weight-vector close to the old one, hoping that it will help to avoid forgetting and facilitate knowledge reuse. The most common is a weight-regularization technique known as Elastic-Weight Consolidation (EWC) (Kirkpatrick et al., 2017), which, at a task t, minimizes the following objective using the previous weight $\boldsymbol{w}_{t-1}$,

$$\ell_t^{\text{weight}}(\boldsymbol{w}) = \sum_{i\in\mathcal{D}_t} \ell\big(y_i, \sigma(f_{\boldsymbol{w}}^i)\big) + \frac{\lambda}{2}(\boldsymbol{w} - \boldsymbol{w}_{t-1})^\top \mathbf{F}_{t-1}(\boldsymbol{w} - \boldsymbol{w}_{t-1}), \tag{3}$$

where the second term is a quadratic regularizer with a weight-importance matrix $\mathbf{F}_{t-1}$, and $\lambda \geq 0$ is a trade-off hyperparameter. The simplest choice of $\mathbf{F}_{t-1}$ is to use the diagonal of a generalized Gauss-Newton (GGN) matrix (Martens, 2020). The GGN is defined as,

$$\mathbf{G}(\mathcal{D}_{1:t}) := \sum_{i\in\mathcal{D}_{1:t}} \left[\nabla f_{\boldsymbol{w}_t}^i\right] \sigma'(f_{\boldsymbol{w}_t}^i) \left[\nabla f_{\boldsymbol{w}_t}^i\right]^\top, \tag{4}$$

where $\nabla f_{\boldsymbol{w}_t}^i$ denotes the Jacobian, that is, derivative of $f_{\boldsymbol{w}}(\boldsymbol{x}_i)$ with respect to $\boldsymbol{w}$ at $\boldsymbol{w} = \boldsymbol{w}_t$, and $\sigma'(f^i)$ denotes the derivative of $\sigma(f)$ with respect to f at $f = f^i$. Often, the regularizer δ is also added to the GGN matrix to reduce ill-conditioning. Computation of $\mathbf{F}_{t-1}$ can be done in an online fashion as the training proceeds over tasks (Schwarz et al., 2018). This method uses a compact representation of the past knowledge as we need to only store $\boldsymbol{w}_{t-1}$ and the diagonal matrix $\mathbf{F}_{t-1}$, requiring $O(P)$ memory. The method is also simple to implement within deep-learning codebases, requiring relatively little overhead. Other choices are possible for the importance matrix (Zenke et al., 2017; Aljundi et al., 2018; Benzing, 2022).

An alternative to regularization-based methods is based on experience replay (Robins, 1995; Shin et al., 2017). Such methods store a subset of past data in a memory $\mathcal{M}_t$ and add it to the new data during training:

$$\ell_t^{\text{er}}(\boldsymbol{w}) = \sum_{i\in\mathcal{D}_t\cup\mathcal{M}_{t-1}} \ell\big(y_i, \sigma(f_{\boldsymbol{w}}^i)\big).$$

This method can be accurate when the memory represents the data well, but this often requires a large memory that grows with the number of tasks.

A popular approach to combine these two previous approaches is to use functional regularization (Titsias et al., 2020; Pan et al., 2020) where, instead of regularizing the weights, we regularize the function outputs at a few past input locations stored in a memory:

$$\ell_t^{\text{func}}(\boldsymbol{w}) = \sum_{i\in\mathcal{D}_t} \ell\big(y_i, \sigma(f_{\boldsymbol{w}}^i)\big) + \frac{\lambda}{2} \sum_{j\in\mathcal{M}_{t-1}} \ell\left(\sigma(f_{\boldsymbol{w}_{t-1}}^j), \sigma(f_{\boldsymbol{w}}^j)\right). \tag{5}$$

Some methods implement this via knowledge-distillation (Rebuffi et al., 2017; Buzzega et al., 2020). Some simply use the original loss while others use the squared loss (Benjamin et al., 2019). An advantage of

functional regularization is that it does not require the labels associated with the inputs in $\mathcal{M}_t$, which enables the use of an arbitrary input $\boldsymbol{x}$ which is not restricted to be from $\mathcal{D}_{1:t}$. For example, we can use a deep generative model to generate pseudo-inputs (Shin et al., 2017), or learn them as in sparse Gaussian processes (Titsias, 2009).

Overall, we see that each method has its own complementary strengths: Weight-regularization is compact, experience replay can be accurate, and functional regularization can use arbitrary memory inputs. Combining these approaches can strike a good balance between performance and memory size, but at present, little has been done to find principled ways to combine them. One could simply add them together, but there are many choices one needs to make. For example, how should we choose the importance matrix and the specific forms of the regularizers? Our goal in this paper is to provide a theoretically-motivated approach to answer such questions.

4 A principle of adaptation: gradient reconstruction of the past

We will use the recently proposed principle of adaptation by Khan & Swaroop (2021) to combine and improve the CL strategies discussed in Section 3. The principle suggests to reconstruct the gradient of the past objective by using a combination of weight and function-space regularizers. Specifically, at task t, we consider minimizing (for some $\tau > 0$)

$$\ell_t^{\text{K-prior}}(\boldsymbol{w}) = \sum_{i \in \mathcal{D}_t} \ell\big(y_i, \sigma(f_{\boldsymbol{w}}^i)\big) + \tau\, \mathcal{K}_t(\boldsymbol{w}; \boldsymbol{w}_{t-1}, \mathcal{M}_{t-1}), \tag{6}$$

where $\mathcal{K}_t(\boldsymbol{w}; \boldsymbol{w}_t, \mathcal{M}_t)$ is a regularizer that combines a weight-space regularizer using $\boldsymbol{w}_t$ and a function-space regularizer over the memory $\mathcal{M}_t$. The regularizer is called the Knowledge-adaptation prior (K-prior), and is designed with the goal to minimize the gradient reconstruction error of the past training objective. We will use $\tau = 1$ unless noted otherwise.

Specifically, at task t, the past training objective is $\ell_{t-1}^{\text{batch}}(\boldsymbol{w})$, and we want to design the prior to minimize the magnitude of the gradient error for all $\boldsymbol{w}$ (see derivation in Appendix A):

$$\boldsymbol{e}_t(\boldsymbol{w}) := \nabla \ell_{t-1}^{\text{batch}}(\boldsymbol{w}) - \nabla \mathcal{K}_t(\boldsymbol{w}; \boldsymbol{w}_{t-1}, \mathcal{M}_{t-1}). \tag{7}$$

The loss $\ell_{t-1}^{\text{batch}}$ depends on all the past data $\mathcal{D}_{1:t-1}$, and our goal is to reconstruct its gradient by using the weight vector $\boldsymbol{w}_{t-1}$ and a memory $\mathcal{M}_{t-1}$. Khan & Swaroop (2021) showed that many existing adaptive strategies in machine learning for one-step adaptation tasks can be recovered from this principle. For example, the following K-prior with $\mathcal{M}_{t-1} = \mathcal{D}_{1:t-1}$ gives zero error $\boldsymbol{e}_t(\boldsymbol{w})$ for generalized-linear models $f_{\boldsymbol{w}}^i = \boldsymbol{x}_i^\top \boldsymbol{w}$:

$$\mathcal{K}_t(\boldsymbol{w}; \boldsymbol{w}_{t-1}, \mathcal{M}_{t-1}) = \sum_{i \in \mathcal{M}_{t-1}} \ell\Big(\sigma(f_{\boldsymbol{w}_{t-1}}^i), \sigma(f_{\boldsymbol{w}}^i)\Big) + \frac{\delta}{2}(\boldsymbol{w} - \boldsymbol{w}_{t-1})^\top (\boldsymbol{w} - \boldsymbol{w}_{t-1}), \tag{8}$$

where $\delta \geq 0$ is the L_2 regularization constant. The K-prior does not use the labels, just like the functional regularization discussed earlier, yet the gradient can be reconstructed by using the predictions at the inputs locations $\boldsymbol{x}_i \in \mathcal{D}_{1:t-1}$. Many other similar results are shown by Khan & Swaroop (2021) for other models, such as support vector machines, Gaussian processes, knowledge distillation, functional-regularization, and the memory-based methods used in continual learning.

While promising, there are still multiple issues with the work of Khan & Swaroop (2021), which we address in this paper. First, they did not consider the sequential setup such as continual learning. Second, the error incurred by their K-prior, of form Eq. (8), is non-zero for neural networks: see Khan & Swaroop (2021, Sec. 4.2). For the continual learning problem, this can be disastrous because errors can accumulate quickly over tasks, deteriorating performance. Third, the weight-regularizer in Eq. (8) ignores the weight importance, which is commonly used in other works (Kirkpatrick et al., 2017; Schwarz et al., 2018; Ritter et al., 2018) and can improve performance.

In this paper, we will address these issues, combining and improving regularization and memory-based methods. We will start with functional-regularization, and then add a weight regularizer and experience replay to decrease its error. This will yield a prior with lower error than each individual method on its own.

5 A new improved K-prior

Using the principle described in the previous section, we will now design a prior that combines a weight regularizer, a functional regularizer, and experience replay (Fig. 1). As described in the previous section, our goal is to minimize the gradient reconstruction error of the past training objective, i.e., the difference in the gradient of the loss for the full batch method and the K-priors loss with limited memory, see Eq. (7). The functional regularizer is based on knowledge distillation, and combined with an EWC-style quadratic regularizer which uses a specific importance vector to minimize the error in the K-prior of Eq. (8). An additional experience-replay term further reduces the error by storing the labels for a subset of the memory set. We will see that each piece contributes to the reduction of a different type of error, and the combination overall gives lower gradient reconstruction error than each individual component.

5.1 The error in the K-prior Eq. (8) when using a limited memory

We start by analyzing the gradient error in the K-prior of Eq. (8) when it is defined with a limited memory $\mathcal{M}_{t-1}$, instead of the full data $\mathcal{D}_{1:t-1}$. As shown in Appendix A, the error is given as follows,

$$\boldsymbol{e}_t(\boldsymbol{w}) = \underbrace{\sum_{i \in \mathcal{D}_{1:t-1} \setminus \mathcal{M}_{t-1}} \nabla f^i_{\boldsymbol{w}} \left[\sigma(f^i_{\boldsymbol{w}}) - \sigma(f^i_{\boldsymbol{w}_{t-1}}) \right]}_{:= \boldsymbol{e}_t^{\text{mem}}(\boldsymbol{w}; \boldsymbol{w}_{t-1}, \mathcal{D}_{1:t-1} \setminus \mathcal{M}_{t-1})} + \underbrace{\sum_{i \in \mathcal{D}_{1:t-1}} \nabla f^i_{\boldsymbol{w}} r^i_{\boldsymbol{w}_{t-1}} + \delta \boldsymbol{w}_{t-1}}_{:= \boldsymbol{e}_t^{\text{NN}}(\boldsymbol{w}; \boldsymbol{w}_{t-1}, \mathcal{D}_{1:t-1})}, \tag{9}$$

where $r^i_{\boldsymbol{w}_t} = \sigma(f^i_{\boldsymbol{w}_t}) - y_i$ is the residual.[1] The first error term $\boldsymbol{e}_t^{\text{mem}}$ arises due to the use of limited memory $\mathcal{M}_{t-1}$, and can be reduced to zero by increasing the memory size to include all past input examples. In contrast, the second error term $\boldsymbol{e}_t^{\text{NN}}$ arises due to the use of neural networks, and reduces only when the network gets better in predicting the past data $\mathcal{D}_{1:t-1}$, that is, when the residuals go to zero. We will now show that $\boldsymbol{e}_t^{\text{mem}}$ can be reduced by adding an EWC-style weight regularizer, while $\boldsymbol{e}_t^{\text{NN}}$ can be reduced by adding an experience replay term with a specific memory.

5.2 Reducing $\mathbf{e}_t^{\text{mem}}$ using an EWC-style regularizer

The error $\boldsymbol{e}_t^{\text{mem}}$ can be reduced by using a first-order Taylor approximation of $\sigma(f^i_w)$ at $\boldsymbol{w}_{t-1}$,

$$\sigma(f^i_{\boldsymbol{w}}) \approx \sigma(f^i_{\boldsymbol{w}_{t-1}}) + \sigma'(f^i_{\boldsymbol{w}_{t-1}}) (\nabla f^i_{\boldsymbol{w}_{t-1}})^\top (\boldsymbol{w} - \boldsymbol{w}_{t-1}). \tag{10}$$

Plugging this into the definition of the error, we get

$$\boldsymbol{e}_t^{\text{mem}} \approx \underbrace{\left[\sum_{i \in \mathcal{D}_{1:t-1} \setminus \mathcal{M}_{t-1}} \left[\nabla f^i_{\boldsymbol{w}_{t-1}} \right] \sigma'(f^i_{\boldsymbol{w}_{t-1}}) \left[\nabla f^i_{\boldsymbol{w}_{t-1}} \right]^\top \right]}_{= \mathbf{G}(\mathcal{D}_{1:t-1} \setminus \mathcal{M}_{t-1})} (\boldsymbol{w} - \boldsymbol{w}_{t-1}),$$

where we use the definition of the GGN matrix given in Eq. (4), and approximate $\nabla f^i_{\boldsymbol{w}_{t-1}} \approx \nabla f^i_{\boldsymbol{w}}$. The right hand side is equal to the gradient of an EWC-style regularizer,

$$\boldsymbol{c}_t^{\text{mem}} = \tfrac{1}{2} (\boldsymbol{w} - \boldsymbol{w}_{t-1})^\top \mathbf{G}(\mathcal{D}_{1:t-1} \setminus \mathcal{M}_{t-1}) (\boldsymbol{w} - \boldsymbol{w}_{t-1}), \tag{11}$$

which uses the GGN over the past data but, importantly, excludes the memory $\mathcal{M}_{t-1}$ from it.[2] We can now define a new K-prior by adding the correction term to Eq. (6), giving,

$$\mathcal{K}_t^{\text{mem}}(\boldsymbol{w}; \boldsymbol{w}_{t-1}, \mathbf{F}_{t-1}, \mathcal{M}_{t-1}) = \sum_{i \in \mathcal{M}_{t-1}} \ell\Big(\sigma(f^i_{\boldsymbol{w}_{t-1}}), \sigma(f^i_{\boldsymbol{w}})\Big) + \tfrac{1}{2} (\boldsymbol{w} - \boldsymbol{w}_{t-1})^\top \mathbf{F}_{t-1} (\boldsymbol{w} - \boldsymbol{w}_{t-1}), \tag{12}$$

[1] Note that the combined error term in (9) unifies the limited memory error term and the neural network error term stated in, respectively, Eq. (11) and Eq. (16) in Khan & Swaroop (2021).

[2] Note that the derivation of (11) follows the derivation of Eq. (12) in Khan & Swaroop (2021).

where we define $\mathbf{F}_{t-1} = \mathbf{G}(\mathcal{D}_{1:t-1} \backslash \mathcal{M}_{t-1}) + \hat{\delta}\mathbf{I}$. By correcting for the error term, this K-prior reduces the error introduced in the K-prior of Eq. (8) due to a limited memory. Similarly to Online EWC, we can use a diagonal approximation to the GGN, and update it online.

The new K-prior not only reduces the gradient error, but also is more general because other regularizers are obtained as special cases by changing the memory. For an empty memory $\mathcal{M}_{t-1} = \emptyset$, it reduces to the EWC regularizer of Eq. (3): the first term in Eq. (12) disappears and the importance $\mathbf{F}_{t-1}$ is the GGN defined over all the past data, plus $\hat{\delta}\mathbf{I}$. On the other hand, when the memory includes all past data, it reduces to the original K-prior in Eq. (8). When using limited memory, the new K-prior combines the functional and weight regularizers in a way to reduce the error in both EWC and the original K-prior.

5.3 Reducing $\mathbf{e}_t^{\mathbf{NN}}$ using experience replay

The $\boldsymbol{e}_t^{\text{NN}}$ term depends on the mistakes made on the past data, and can be corrected by including an additional memory, denoted by $\mathcal{M}_{2,t-1}$, of the past data where mistakes are significant. We first note that the error is equivalent to the gradient of the following,

$$\boldsymbol{c}_t^{\text{NN}} := \sum_{i \in \mathcal{M}_{2,t-1}} f_{\boldsymbol{w}}^i r_{\boldsymbol{w}_{t-1}}^i + \tfrac{1}{2}\delta \boldsymbol{w}^\top \boldsymbol{w}_{t-1}, \tag{13}$$

when $\mathcal{M}_{2,t-1}$ is set to all the past data. Therefore, by adding $\mathcal{K}_t^{\text{NN}} = \mathcal{K}_t + \boldsymbol{c}_t^{\text{NN}}$ with a subset of past data $\mathcal{M}_{2,t-1}$, we reduce the error simply to $\sum_{i \in \mathcal{D}_{1:t-1} \backslash \mathcal{M}_{2,t-1}} \left[\nabla f_{\boldsymbol{w}}^i r_{\boldsymbol{w}_{t-1}}^i \right]$.

5.4 K-prior with EWC-style regularizer and experience replay

Our new improved K-prior is obtained by simply correcting the K-prior from Eq. (8) by adding the correction terms from Eq. (11) and Eq. (13), that is,

$$\mathcal{K}_t^{\text{new}} = \mathcal{K}_t + \boldsymbol{c}_t^{\text{NN}} + \boldsymbol{c}_t^{\text{mem}} = \sum_{i \in \mathcal{M}_{t-1}} \ell\left(\sigma(f_{\boldsymbol{w}_{t-1}}^i), \sigma(f_{\boldsymbol{w}}^i)\right) + \sum_{i \in \mathcal{M}_{2,t-1}} f_{\boldsymbol{w}}^i r_{\boldsymbol{w}_{t-1}}^i \tag{14}$$

$$+ \tfrac{1}{2}\delta \boldsymbol{w}^\top \boldsymbol{w}_{t-1} + \tfrac{1}{2}(\boldsymbol{w} - \boldsymbol{w}_{t-1})^\top \mathbf{F}_{t-1}(\boldsymbol{w} - \boldsymbol{w}_{t-1}). \tag{15}$$

We make a specific choice of the memory: we choose $\mathcal{M}_{2,t-1}$ to be a subset of $\mathcal{M}_{t-1}$. This, as we show now, simplifies the computation and brings experience replay into our new K-prior.

Consider the first two terms from our improved K-prior in Eq. (14),

$$\sum_{i \in \mathcal{M}_{t-1}} \ell\left(\sigma(f_{\boldsymbol{w}_{t-1}}^i), \sigma(f_{\boldsymbol{w}}^i)\right) + \sum_{i \in \mathcal{M}_{2,t-1}} f_{\boldsymbol{w}}^i r_{\boldsymbol{w}_{t-1}}^i.$$

The gradient of these two terms can be simplified when the second memory is a subset of the first one,

$$\begin{aligned}
&\nabla \left[\sum_{i \in \mathcal{M}_{t-1}} \ell\left(\sigma(f_{\boldsymbol{w}_{t-1}}^i), \sigma(f_{\boldsymbol{w}}^i)\right) + \sum_{i \in \mathcal{M}_{2,t-1}} f_{\boldsymbol{w}}^i r_{\boldsymbol{w}_{t-1}}^i \right] \\
&= \sum_{i \in \mathcal{M}_{t-1}} \nabla f_{\boldsymbol{w}}^i \left[\sigma(f_{\boldsymbol{w}}^i) - \sigma(f_{\boldsymbol{w}_{t-1}}^i) \right] + \sum_{i \in \mathcal{M}_{2,t-1}} \nabla f_{\boldsymbol{w}}^i r_{\boldsymbol{w}_{t-1}}^i \\
&= \sum_{i \in \mathcal{M}_{t-1} \backslash \mathcal{M}_{2,t-1}} \nabla f_{\boldsymbol{w}}^i \left[\sigma(f_{\boldsymbol{w}}^i) - \sigma(f_{\boldsymbol{w}_{t-1}}^i) \right] + \sum_{i \in \mathcal{M}_{2,t-1}} \nabla f_{\boldsymbol{w}}^i \left[\sigma(f_{\boldsymbol{w}}^i) - \sigma(f_{\boldsymbol{w}_{t-1}}^i) \right] + \nabla f_{\boldsymbol{w}}^i r_{\boldsymbol{w}_{t-1}}^i \\
&= \sum_{i \in \mathcal{M}_{t-1} \backslash \mathcal{M}_{2,t-1}} \nabla f_{\boldsymbol{w}}^i \left[\sigma(f_{\boldsymbol{w}}^i) - \sigma(f_{\boldsymbol{w}_{t-1}}^i) \right] + \sum_{i \in \mathcal{M}_{2,t-1}} \nabla f_{\boldsymbol{w}}^i \left[\sigma(f_{\boldsymbol{w}}^i) - y_i) \right]
\end{aligned}$$

where in the second line we used the expression in Eq. (18) for the gradient of the (exponential-family) loss, and where in the last line we used the definition of the residual $r_{\boldsymbol{w}_t}^i = \sigma(f_{\boldsymbol{w}_t}^i) - y_i$ to simplify. This gradient

is equal to the gradient of a sum of a functional-regularizer term and an experience replay term,

$$\sum_{i \in \mathcal{M}_{t-1} \backslash \mathcal{M}_{2,t-1}} \ell\left(\sigma(f^i_{\boldsymbol{w}_{t-1}}), \sigma(f^i_{\boldsymbol{w}})\right) + \sum_{i \in \mathcal{M}_{2,t-1}} \ell\big(y_i, \sigma(f^i_{\boldsymbol{w}})\big)\,, \tag{16}$$

again using the expression for the loss gradient in Eq. (18). Therefore, we can rewrite the new K-prior as the following combination,

$$\begin{aligned}\mathcal{K}^{\text{new}}_t(\boldsymbol{w}; \boldsymbol{w}_{t-1}, \mathbf{F}_{t-1}, \mathcal{M}_{t-1}) = & \underbrace{\sum_{i \in \mathcal{M}_{1,t-1}} \ell\Big(\sigma(f^i_{\boldsymbol{w}_{t-1}}), \sigma(f^i_{\boldsymbol{w}})\Big)}_{\text{Functional-regularization}} + \underbrace{\sum_{i \in \mathcal{M}_{2,t-1}} \ell\big(y_i, \sigma(f^i_{\boldsymbol{w}})\big)}_{\text{Experience replay}} \\ & + \underbrace{\tfrac{1}{2}(\boldsymbol{w} - \boldsymbol{w}_{t-1})^\top \mathbf{F}_{t-1}(\boldsymbol{w} - \boldsymbol{w}_{t-1}) + \tfrac{1}{2}\delta \boldsymbol{w}^\top \boldsymbol{w}_{t-1}}_{\text{Weight-regularization}},\end{aligned} \tag{17}$$

where $\mathcal{M}_{1,t-1} = \mathcal{M}_{t-1} \backslash \mathcal{M}_{2,t-1}$ and $\mathcal{M}_{2,t-1}$ are two disjoint subsets of the memory, and where we define $\mathbf{F}_{t-1} = \mathbf{G}(\mathcal{D}_{1:t-1} \backslash \mathcal{M}_{t-1}) + \delta \mathbf{I}$. The new prior combines a weight regularizer, a functional regularizer, and experience replay. The functional regularizer is based on knowledge distillation, and combined with an EWC-style quadratic regularizer which uses an importance vector obtained over all the past data but excluding the memory $\mathcal{M}_{t-1} = \mathcal{M}_{1,t-1} \cup \mathcal{M}_{2,t-1}$. Using this combination, the new prior gives lower gradient reconstruction error than each method alone.

In our experiments, we select the memories as follows. We first randomly (uniformly) sample the memory set $\mathcal{M}_{t-1}$ from all data $\mathcal{D}_{1:t-1}$, and then randomly split it into the two memory subsets $\mathcal{M}_{1,t-1}$ and $\mathcal{M}_{2,t-1}$; for simplicity, we use equally sized subsets, i.e., $|\mathcal{M}_{1,t-1}| = |\mathcal{M}_{2,t-1}|$. We found this simple selection strategy to work surprisingly well, and leave the study of more sophisticated approaches (as well as of settings where $|\mathcal{M}_{1,t-1}| \neq |\mathcal{M}_{2,t-1}|$) for future work.

6 Empirical evaluation

We first describe the general experimental setup used throughout our evaluation. We then present empirical results corroborating the practical efficacy of our proposed `Kprior+EWC+Replay` method. We focus on multi-class classification in the task-incremental learning setting. In particular, we evaluate on three continual learning benchmarks with increasing size and thus difficulty: 1) Split-CIFAR (medium-scale), 2) Split-TinyImageNet (medium-to-large-scale), and 3) ImageNet-1000 (large-scale). See Appendix B for more details on the experiments (e.g. hyperparameters used).

6.1 Experimental setup

Continual learning setup. We mostly follow previous works on CL. We consider the common multi-head task-incremental (Van de Ven & Tolias, 2019) setting with known task identities: each method is trained sequentially on all tasks with a separate classification head per task, and is told which task an input belongs to both at train and test time. We report test accuracy of the final model trained on the entire task sequence (averaged over the test sets of all observed tasks). We also compute average forgetting (aka backward-transfer) as defined in Lopez-Paz & Ranzato (2017), which captures the (average) difference in accuracy between when a task is first trained and after the final task. We plot mean $\pm$ standard error over three seeds, and assess performance across a wide range of memory sizes.

Methods. In addition to our proposed `Kprior+EWC+Replay` method, we evaluate four relevant baselines for comparison. As our method combines Kprior with both EWC and experience replay, we also do ablations to assess the benefit of either term alone. In summary, we consider the following methods:

1. **`Kprior+EWC+Replay`**. Our proposed regularizer which combines the K-prior function regularizer over $\mathcal{M}_1$ with the EWC-style weight regularizer and the experience replay term over $\mathcal{M}_2$.
2. `Kprior`. The original K-prior regularizer over $\mathcal{M}_1$ as proposed by Khan & Swaroop (2021), *without* the EWC-style weight regularization term and *without* the experience replay term over $\mathcal{M}_2$.

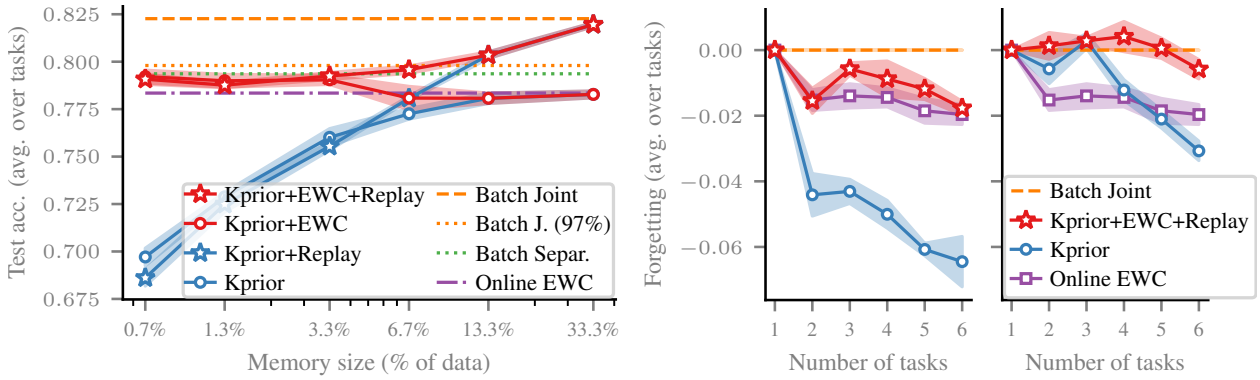

Figure 2: **Results on Split-CIFAR.** `Kprior+EWC+Replay` is superior across memory sizes, closely approaching `Batch Joint` for memory size 33.3% (left; x-axis log-scaled). It also forgets less (relative to `Batch Joint`) with a growing number of tasks, for memory sizes 0.7% (middle) and 33.3% (right).

3. `Kprior+EWC` (ablation). A regularizer combining the K-prior function regularizer over $\mathcal{M}_1$ with *only* the EWC-style weight regularization, i.e. *without* the experience replay term over $\mathcal{M}_2$.
4. `Kprior+Replay` (ablation). A regularizer combining the K-prior function regularizer over $\mathcal{M}_1$ with *only* the experience replay term over $\mathcal{M}_2$, i.e. *without* the EWC-style weight regularization.
5. `Batch Joint`. Joint batch training of a single multi-head model across the data of all tasks, i.e. the optimal CL solution which serves as an upper bound we wish to approach.
6. `Batch Separate`. Independent batch training of a *separate* model for each task.
7. `Online EWC` (Schwarz et al., 2018), which has the same weight regularizer as Kprior+ EWC+Replay, but *without* the function regularizer over $\mathcal{M}_1$ or the experience replay term over $\mathcal{M}_2$.

6.2 Results on Split-CIFAR

Setup. Split-CIFAR (Zenke et al., 2017) has 6 tasks with 10 classes each. The first task is CIFAR-10 (Krizhevsky et al., 2009) with 50,000 training and 10,000 test data points across 10 classes. The subsequent 5 tasks are taken sequentially from CIFAR-100 (Krizhevsky et al., 2009), each with 5,000 training and 1,000 test data points across 10 classes. In total, we thus have 90,000 data points. We use the same CifarNet model as Zenke et al. (2017); Pan et al. (2020): a multi-head CNN with 4 convolutional layers, followed by 2 dense layers with dropout, with ∼1.2M model parameters in total. On each task, we train for 80 epochs using Adam with learning rate 10^{-3} and batch size 256.

Results. Fig. 2 shows our results on Split-CIFAR. We consider memory sizes between 100 and 5,000 per task; at 5,000, we thus store 10% of the data for task 1, and all data for tasks 2-5 (which in total thus corresponds to a third of all data). We see that `Kprior` performs poorly at small memory sizes and is much worse than `Online EWC`. While performance improves noticeably with growing memory size, `Kprior` remains far below `Batch Joint` even at memory size 33.3%. This confirms that when using a NN instead of a GLM, the theory behind `Kprior` (see Section 4) indeed ceases to hold. However, when we add the experience replay term to correct for that error (`Kprior+Replay`), performance is substantially boosted at large memory sizes, actually enabling us to reach `Batch Joint` performance for memory size 33.3%. However, the experience replay correction term does not help at small memory sizes. In contrast, adding the EWC-style weight regularizer (`Kprior+EWC`) substantially improves performance at small memory sizes, empirically confirming the property that `Kprior+EWC` converges to `Online EWC` for small memories (see Section 5.2). However, we also confirm that for large memories, `Kprior+EWC` converges to `Kprior`, resulting in a performance drop.

Finally, we see that `Kprior+EWC+Replay` obtains ∼97% of the batch performance with just ∼10% of the data (and full batch performance with ∼33.3% of the data), but does not degrade as memory size decreases (unlike `Kprior+Replay`). `Kprior+EWC+Replay` thus combines the complementary benefits of both

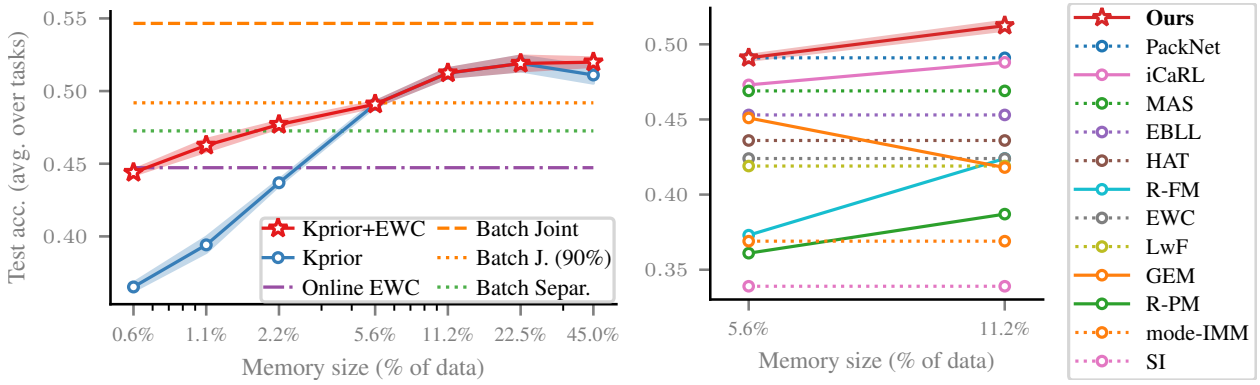

Figure 3: **Results on Split-TinyImageNet.** `Kprior+EWC` performs well across memory sizes (left; x-axis log-scaled) and compared to further strong baselines from Delange et al. (2021) (right).

error correction terms, i.e. of both EWC-style weight-regularization and experience replay, to significantly improve upon vanilla `Kprior` in both the small *and* large memory regime. Fig. 2 (mid & right) further shows that our method can leverage prior knowledge more effectively than other methods, thereby suffering less from forgetting with a growing number of tasks. This confirms that the two error correction terms in `Kprior+EWC+Replay` are particularly important for mitigating error accumulation across longer task sequences.

6.3 Results on Split-TinyImageNet

Setup. Following Delange et al. (2021), we construct Split-TinyImageNet by dividing TinyImageNet (Le & Yang, 2015) into a sequence of 10 tasks with 20 classes each (using the same random division as in Delange et al. (2021)). Each class has 500 data points split into training (80%) and validation (20%), and 50 test points (totalling to 110,000 points). We use the VGG-like BASE model from Delange et al. (2021) with 6 convolutional layers, 4 max pooling layers, and 2 dense layers, with a total of $\sim$3.5M parameters. On each task, we train for 70 epochs (with early stopping and exponential learning rate decay, without regularization) using SGD with momentum 0.9 and batch size 200. This replicates the setup of Delange et al. (2021) to make our results directly comparable.[3]

Results. Fig. 3 shows our results on Split-TinyImageNet. We found that the experience replay error correction term does not help on this benchmark, so we representatively plot just `Kprior` and `Kprior+EWC`.[4] We again see that `Kprior+EWC` can substantially improve over `Kprior` (especially at small memory sizes) and `Online EWC`, achieving $\sim$90% of the batch performance with $\sim$10% of the data (Fig. 3 left). It also compares favourably against a diverse range of other strong CL methods across all three CL paradigms: 1) memory/rehearsal – iCaRL (Rebuffi et al., 2017), GEM (Lopez-Paz & Ranzato, 2017), R-FM & R-PM (Delange et al., 2021), 2) weight-regularization – LwF (Li & Hoiem, 2017), EBLL (Rannen et al., 2017), EWC (Kirkpatrick et al., 2017), SI (Zenke et al., 2017), MAS (Aljundi et al., 2018), mode-IMM (Lee et al., 2017), and 3) architectural – PackNet (Mallya & Lazebnik, 2018), HAT (Serra et al., 2018) (Fig. 3 right).[5]

6.4 Results on ImageNet-1000

Setup. We consider the ImageNet-1000 benchmark proposed by Rebuffi et al. (2017), which randomly splits the full ImageNet dataset (Deng et al., 2009) of $\sim$1.2M data points into a sequence of 10 tasks with 100 classes and $\sim$120K data points each. Following Rebuffi et al. (2017), we use a ResNet-18 with $\sim$11M model

[3]The only difference lies in the hyperparameter tuning procedure: while Delange et al. (2021) use their proposed online tuning algorithm, we resort to a standard grid search for simplicity; see Appendix B for details.

[4]This is likely because almost perfect train accuracy is attained on all tasks (see e.g. Table 14 in Delange et al. (2021)). Thus, $\boldsymbol{e}_t^{\text{NN}}$ in Eq. (9) is close to zero, such that NN error correction cannot boost performance.

[5]Results are from Delange et al. (2021); their total memory sizes $[4500, 9000]$ correspond to $[5.6\%, 11.2\%]$ of the data.

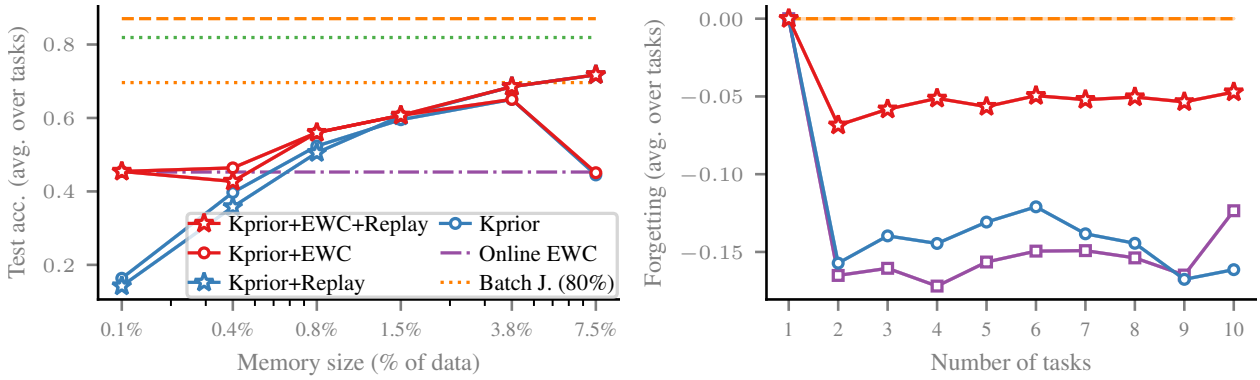

Figure 4: **Results on ImageNet-1000.** `Kprior+EWC+Replay` performs favorably across a range of memory sizes (left; x-axis log-scaled), and suffers less from forgetting (relative to `Batch Joint`) with an increasing number of tasks, here exemplary shown at the largest memory size of 7.5% (right).

parameters. For training on each task, we use the ImageNet reference training pipeline (with 40 epoch configuration) of the FFCV library (Leclerc et al., 2022).[6]

Results. Fig. 4 shows our results on ImageNet-1000. We consider memory sizes between 200 and 10K per task, where the latter amounts to 7.5% of the entire data. The observed trends qualitatively match those from previous experiments. In particular, `Kprior` underperforms for small memory sizes, and while it improves with increasing memory, it peaks at a 3.8% memory and then even starts declining. We hypothesize that this is again due to accumulation of the NN error, which might become more severe with a larger memory as more data points can contribute to the error. This is evidenced by the fact that correcting for the NN error (`Kprior+Replay`) substantially boosts performance at a 7.5% memory (but it remains poor at small memories). In contrast, `Kprior+EWC` again improves accuracy only for small memories. Finally, `Kprior+EWC+Replay` combines the benefit of both error correction terms to perform well across all memory sizes, achieving $>80\%$ of the batch performance with a memory of $<10\%$ of the past data. It also again forgets less along the task sequence, demonstrating that it better mitigates error accumulation.

7 Conclusion

In this work, we proposed to address the continual learning problem in a theoretically-grounded way by explicitly approximating the optimal model obtained via batch-training on all tasks jointly. To this end, we developed `Kprior+EWC+Replay`, a new continual learning method which efficiently re-uses prior knowledge to reconstruct the gradients of the past training objective as faithfully as possible. To achieve this, our method combines principles from function-regularization, weight-regularization, and experience replay to reduce the gradient-reconstruction error. Empirically, we demonstrated the effectiveness and scalability of `Kprior+EWC+Replay` across different memory sizes on common task-incremental continual learning benchmarks. In particular, we showed that our proposed approach can be less susceptible to catastrophic forgetting and thus achieve better performance compared to various baselines. Notably, our method can achieve $>80\%$ of the batch performance by utilizing a memory of $<10\%$ of the past data on the task-incremental continual learning benchmarks considered. For future work, we aim to investigate how more sophisticated strategies for selecting the two memory sets can further boost performance of our method.

References

Rahaf Aljundi, Francesca Babiloni, Mohamed Elhoseiny, Marcus Rohrbach, and Tinne Tuytelaars. Memory aware synapses: Learning what (not) to forget. In *Proceedings of the European Conference on Computer Vision (ECCV)*, pp. 139–154, 2018.

[6]For all details of the training procedure, see `https://github.com/libffcv/ffcv-imagenet/`.

Ari S Benjamin, David Rolnick, and Konrad Kording. Measuring and regularizing networks in function space. *International Conference on Learning Representation*, 2019.

Frederik Benzing. Unifying importance based regularisation methods for continual learning. In *International Conference on Artificial Intelligence and Statistics*, pp. 2372–2396. PMLR, 2022.

Pietro Buzzega, Matteo Boschini, Angelo Porrello, Davide Abati, and Simone Calderara. Dark experience for general continual learning: a strong, simple baseline. *Advances in neural information processing systems*, 33:15920–15930, 2020.

Matthias Delange, Rahaf Aljundi, Marc Masana, Sarah Parisot, Xu Jia, Ales Leonardis, Greg Slabaugh, and Tinne Tuytelaars. A continual learning survey: Defying forgetting in classification tasks. *IEEE Transactions on Pattern Analysis and Machine Intelligence*, 2021.

Jia Deng, Wei Dong, Richard Socher, Li-Jia Li, Kai Li, and Li Fei-Fei. Imagenet: A large-scale hierarchical image database. In *2009 IEEE conference on computer vision and pattern recognition*, pp. 248–255. Ieee, 2009.

Tom Diethe, Tom Borchert, Eno Thereska, Borja Balle, and Neil Lawrence. Continual learning in practice. In *NeurIPS 2018 workshop on Continual Learning*, 2019.

Mohammad Emtiyaz Khan and Siddharth Swaroop. Knowledge-adaptation priors. *Advances in neural information processing systems*, 2021.

James Kirkpatrick, Razvan Pascanu, Neil Rabinowitz, Joel Veness, Guillaume Desjardins, Andrei A Rusu, Kieran Milan, John Quan, Tiago Ramalho, Agnieszka Grabska-Barwinska, et al. Overcoming catastrophic forgetting in neural networks. *Proceedings of the national academy of sciences*, 114(13):3521–3526, 2017.

Alex Krizhevsky, Geoffrey Hinton, et al. Learning multiple layers of features from tiny images. Technical report, Citeseer, 2009.

Ya Le and Xuan Yang. Tiny imagenet visual recognition challenge. *CS 231N*, 7(7):3, 2015.

Guillaume Leclerc, Andrew Ilyas, Logan Engstrom, Sung Min Park, Hadi Salman, and Aleksander Madry. ffcv. `https://github.com/libffcv/ffcv/`, 2022. commit f25386557e213711cc8601833add36ff966b80b2.

Sang-Woo Lee, Jin-Hwa Kim, Jaehyun Jun, Jung-Woo Ha, and Byoung-Tak Zhang. Overcoming catastrophic forgetting by incremental moment matching. *Advances in neural information processing systems*, 30, 2017.

Zhizhong Li and Derek Hoiem. Learning without forgetting. *IEEE transactions on pattern analysis and machine intelligence*, 40(12):2935–2947, 2017.

David Lopez-Paz and Marc'Aurelio Ranzato. Gradient episodic memory for continual learning. In *Advances in Neural Information Processing Systems*, pp. 6467–6476, 2017.

Arun Mallya and Svetlana Lazebnik. Packnet: Adding multiple tasks to a single network by iterative pruning. In *Proceedings of the IEEE conference on Computer Vision and Pattern Recognition*, pp. 7765–7773, 2018.

James Martens. New insights and perspectives on the natural gradient method. *The Journal of Machine Learning Research*, 21(1):5776–5851, 2020.

Martial Mermillod, Aurélia Bugaiska, and Patrick Bonin. The stability-plasticity dilemma: Investigating the continuum from catastrophic forgetting to age-limited learning effects. *Frontiers in psychology*, 4:504, 2013.

Cuong V Nguyen, Yingzhen Li, Thang D Bui, and Richard E Turner. Variational continual learning. *International Conference on Learning Representation*, 2018.

Andrei Paleyes, Raoul-Gabriel Urma, and Neil D Lawrence. Challenges in deploying machine learning: a survey of case studies. *arXiv preprint arXiv:2011.09926*, 2020.

Pingbo Pan, Siddharth Swaroop, Alexander Immer, Runa Eschenhagen, Richard E. Turner, and Mohammad Emtiyaz Khan. Continual deep learning by functional regularisation of memorable past. *Advances in neural information processing systems*, 2020.

German I Parisi, Ronald Kemker, Jose L Part, Christopher Kanan, and Stefan Wermter. Continual lifelong learning with neural networks: A review. *Neural Networks*, 113:54–71, 2019.

Amal Rannen, Rahaf Aljundi, Matthew B Blaschko, and Tinne Tuytelaars. Encoder based lifelong learning. In *Proceedings of the IEEE International Conference on Computer Vision*, pp. 1320–1328, 2017.

Sylvestre-Alvise Rebuffi, Alexander Kolesnikov, Georg Sperl, and Christoph H Lampert. iCaRL: Incremental classifier and representation learning. In *Proceedings of the IEEE conference on Computer Vision and Pattern Recognition*, pp. 2001–2010, 2017.

Hippolyt Ritter, Aleksandar Botev, and David Barber. Online structured Laplace approximations for overcoming catastrophic forgetting. In *Advances in Neural Information Processing Systems*, pp. 3738–3748, 2018.

Anthony Robins. Catastrophic forgetting, rehearsal and pseudorehearsal. *Connection Science*, 7(2):123–146, 1995.

Jonathan Schwarz, Wojciech Czarnecki, Jelena Luketina, Agnieszka Grabska-Barwinska, Yee Whye Teh, Razvan Pascanu, and Raia Hadsell. Progress & compress: A scalable framework for continual learning. In *Proceedings of Machine Learning Research*. PMLR, 2018.

Joan Serra, Didac Suris, Marius Miron, and Alexandros Karatzoglou. Overcoming catastrophic forgetting with hard attention to the task. In *International Conference on Machine Learning*, pp. 4548–4557. PMLR, 2018.

Hanul Shin, Jung Kwon Lee, Jaehong Kim, and Jiwon Kim. Continual learning with deep generative replay. In *Advances in neural information processing systems*, 2017.

Richard Sutton. Two problems with back propagation and other steepest descent learning procedures for networks. In *Proceedings of the Eighth Annual Conference of the Cognitive Science Society, 1986*, pp. 823–832, 1986.

Siddharth Swaroop. *Probabilistic Continual Learning using Neural Networks*. PhD thesis, University of Cambridge, 2022.

Michalis Titsias. Variational learning of inducing variables in sparse gaussian processes. In *Artificial intelligence and statistics*, pp. 567–574. PMLR, 2009.

Michalis K Titsias, Jonathan Schwarz, Alexander G de G Matthews, Razvan Pascanu, and Yee Whye Teh. Functional regularisation for continual learning using Gaussian processes. *International Conference on Learning Representation*, 2020.

Gido M Van de Ven and Andreas S Tolias. Three scenarios for continual learning. *arXiv preprint arXiv:1904.07734*, 2019.

Vladimir Vapnik, Rauf Izmailov, et al. Learning using privileged information: similarity control and knowledge transfer. *J. Mach. Learn. Res.*, 16(1):2023–2049, 2015.

Friedemann Zenke, Ben Poole, and Surya Ganguli. Continual learning through synaptic intelligence. In *International Conference on Machine Learning*, pp. 3987–3995. PMLR, 2017.

A Derivation of error for K-priors with limited memory Eq. (9)

Recall that $f^i_{\boldsymbol{w}} = f_{\boldsymbol{w}}(\boldsymbol{x}_i)$ is a shorthand for the model outputs. For ease-of-notation, we will also use the shorthand $\sigma^i_{\boldsymbol{w}} = \sigma(f^i_{\boldsymbol{w}}) = \sigma(f_{\boldsymbol{w}}(\boldsymbol{x}_i))$ for the model predictions. Consider the following expression for the gradient of the (exponential-family) loss (Khan & Swaroop, 2021),

$$\nabla \ell(y_i, \sigma(f^i_{\boldsymbol{w}})) = \nabla f^i_{\boldsymbol{w}} \left[\sigma(f^i_{\boldsymbol{w}}) - y_i\right]. \tag{18}$$

We start by deriving the gradient error in (7),

$$\begin{aligned}
&\nabla \ell_t^{\text{batch}}(\boldsymbol{w}) - \nabla \ell_t^{\text{K-prior}}(\boldsymbol{w}) \\
&= \nabla \left(\ell_t^{\text{batch}}(\boldsymbol{w}) - \ell_t^{\text{K-prior}}(\boldsymbol{w})\right) \\
&\overset{(1),(6)}{=} \nabla \left(\sum_{i\in\mathcal{D}_t} \ell\left(y_i, \sigma^i_{\boldsymbol{w}}\right) + \ell_{t-1}^{\text{batch}}(\boldsymbol{w}) - \sum_{i\in\mathcal{D}_t} \ell\left(y_i, \sigma^i_{\boldsymbol{w}}\right) - \mathcal{K}(\boldsymbol{w}; \boldsymbol{w}_{t-1}, \mathcal{M})\right) \\
&= \nabla \left(\ell_{t-1}^{\text{batch}}(\boldsymbol{w}) - \mathcal{K}(\boldsymbol{w}; \boldsymbol{w}_{t-1}, \mathcal{M})\right).
\end{aligned}$$

To obtain We then have,

$$\begin{aligned}
&\nabla \left(\ell_{t-1}^{\text{batch}}(\boldsymbol{w}) - \mathcal{K}(\boldsymbol{w}; \boldsymbol{w}_{t-1}, \mathcal{M})\right) \\
&\overset{(1),(8)}{=} \nabla \left(\sum_{i\in\mathcal{D}_{1:t-1}} \ell\left(y_i, \sigma^i_{\boldsymbol{w}}\right) - \sum_{i\in\mathcal{M}} \ell\left(\sigma^i_{\boldsymbol{w}_{t-1}}, \sigma^i_{\boldsymbol{w}}\right) + \tfrac{1}{2}\delta\|\boldsymbol{w}_{t-1}\|^2\right) \\
&= \sum_{i\in\mathcal{D}_{1:t-1}} \nabla \ell\left(y_i, \sigma^i_{\boldsymbol{w}}\right) - \sum_{i\in\mathcal{M}} \nabla \ell\left(\sigma^i_{\boldsymbol{w}_{t-1}}, \sigma^i_{\boldsymbol{w}}\right) + \delta \boldsymbol{w}_{t-1} \\
&\overset{(18)}{=} \sum_{i\in\mathcal{D}_{1:t-1}} \nabla f^i_{\boldsymbol{w}} \left[\sigma^i_{\boldsymbol{w}} - y_i\right] - \sum_{i\in\mathcal{M}} \nabla f^i_{\boldsymbol{w}} \left[\sigma^i_{\boldsymbol{w}} - \sigma^i_{\boldsymbol{w}_{t-1}}\right] + \delta \boldsymbol{w}_{t-1} \\
&= \sum_{i\in\mathcal{D}_{1:t-1}} \nabla f^i_{\boldsymbol{w}} \left[\sigma^i_{\boldsymbol{w}} - y_i + \sigma^i_{\boldsymbol{w}_{t-1}} - \sigma^i_{\boldsymbol{w}} + \sigma^i_{\boldsymbol{w}} - \sigma^i_{\boldsymbol{w}_{t-1}}\right] - \sum_{i\in\mathcal{M}} \nabla f^i_{\boldsymbol{w}} \left[\sigma^i_{\boldsymbol{w}} - \sigma^i_{\boldsymbol{w}_{t-1}}\right] + \delta \boldsymbol{w}_{t-1} \\
&= \sum_{i\in\mathcal{D}_{1:t-1}} \nabla f^i_{\boldsymbol{w}} \left[\sigma^i_{\boldsymbol{w}_{t-1}} - y_i\right] + \sum_{i\in\mathcal{D}_{1:t-1}} \nabla f^i_{\boldsymbol{w}} \left[\sigma^i_{\boldsymbol{w}} - \sigma^i_{\boldsymbol{w}_{t-1}}\right] - \sum_{i\in\mathcal{M}} \nabla f^i_{\boldsymbol{w}} \left[\sigma^i_{\boldsymbol{w}} - \sigma^i_{\boldsymbol{w}_{t-1}}\right] + \delta \boldsymbol{w}_{t-1} \\
&= \sum_{i\in\mathcal{D}_{1:t-1}\setminus\mathcal{M}} \nabla f^i_{\boldsymbol{w}} \left[\sigma^i_{\boldsymbol{w}} - \sigma^i_{\boldsymbol{w}_{t-1}}\right] + \sum_{i\in\mathcal{D}_{1:t-1}} \nabla f^i_{\boldsymbol{w}} \left[\sigma^i_{\boldsymbol{w}_{t-1}} - y_i\right] + \delta \boldsymbol{w}_{t-1} \\
&= \sum_{i\in\mathcal{D}_{1:t-1}\setminus\mathcal{M}} \nabla f^i_{\boldsymbol{w}} \left[\sigma^i_{\boldsymbol{w}} - \sigma^i_{\boldsymbol{w}_{t-1}}\right] + \sum_{i\in\mathcal{D}_{1:t-1}} \nabla f^i_{\boldsymbol{w}} r^i_{\boldsymbol{w}_{t-1}} + \delta \boldsymbol{w}_{t-1}
\end{aligned}$$

where $r^i_{\boldsymbol{w}_{t-1}} = \sigma^i_{\boldsymbol{w}_{t-1}} - y_i$ is the residual of the i'th input using the past model parameters $\boldsymbol{w}_{t-1}$.[7]

B Experiment details

For all methods in all experiments, we tuned hyperparameters in the common way by conducting a (exponentially-spaced) grid search and evaluating performance on a held-out validation set. In particular, we tune the following hyperparameters: a temperature parameter T to scale the logits in the experience replay term (as commonly-done in knowledge distillation, see Khan & Swaroop (2021) for a discussion), a trade-off parameter τ in front of the K-prior-style function regularization term, and a trade-off parameter λ in front of the EWC-style weight regularization term.

We used the following tuned values for those hyperparameters: for Split-CIFAR, we have $T = 2.0$ for all methods, $\tau = 0.1$ for Kprior and Kprior+Replay, $\tau = 0.25$ and $\lambda = 2.0$ for Kprior+EWC and

[7]Note that this derivation follows the derivation in Appendix C in Khan & Swaroop (2021).

Kprior+EWC+Replay, and $\lambda = 10.0$ for Online EWC. For Split-TinyImageNet, we have $T = 1.0$ and $\tau = 16.0$ for all methods. We found that a fixed λ across tasks does not work well for this benchmark, so we tuned a separate λ per task, resulting in the sequence $[330, 85, 45, 30, 20, 15, 10, 10]$ for all methods. In contrast to our grid search procedure, Delange et al. (2021) use a dedicated iterative hyperparameter tuning strategy that trades-off plasticity vs. stability. For ImageNet, we used $T = 1.0$, $\lambda = 1.0$ and $\tau = 0.16$ for all methods.